2 Polarimetry: From Point-Source to Imaging Polarimeters

Biologists dealing with polarization sensitivity of animals, or engineers designing robots using polarization-sensitive imaging detectors to enhance the contrast of objects, for example, need a technique to measure the spatial distribution of polarization in the optical environment. In the 1980's, 1990's and early 2000's, different kinds of imaging polarimetry have been developed to measure the polarization patterns of objects and natural scenes in a wide field of view. The conventional non-imaging point-source polarimeters average polarization over an area of a few degrees only. The conception of "polarization imagery" or "imaging polarimetry" was introduced by Walraven (1977, 1981), capitalizing on the commercial availability of relatively low-cost products and processes to obtain high-resolution information about the polarized components of the skylight radiance. There are two different approaches to build imaging polarimeters:

1. either using a point-source polarimeter with a scanning unit (e.g. Dreher et al. 1992),
2. or substituting the routinely used point-source photodetector by a camera (e.g. Pezzaniti and Chipman 1995).

As a further development of the latter technique, the addition of depth to two-dimensional pictures displaying the spatial distribution of polarization was realized by Mizera et al. (2001), who designed one kind of stereo video polarimetry to measure and visualize in three dimensions the polarization patterns in nature and to mimic the ability of animal eyes to receive visual information from a binocular field of view. Table 2.1 summarizes the most important properties of imaging polarimeters built by different researchers and used for various purposes. In Chapters 2-6 these imaging polarimeters are briefly described after a short introduction into the basic elements of polarimetry and its evolution.

Imaging polarimetry can be efficiently used in all fields of basic research, technology and industry, where the state of polarization of light is an important information. Below some possible applications of polarization are listed, where also imaging polarimetry is routinely used or could be applied in the future:

- stereo cinematography
- studying animal polarization sensitivity
- astronomy (e.g. Gehrels 1974), solar physics (e.g. Beckers and Wagner 1970), spectroscopy (e.g. Kliger et al. 1990), radar polarimetry (e.g. Boerner et al. 1992)
- aerial reconnaissance and automatic target recognition, camouflage breaking (e.g. detections of camouflaged tanks or mines) (e.g. Cariou et al. 1990)
- remote sensing of oil on sea waters (Kondratyev et al. 1974): The detection of regions of the sea surface polluted by an oil film can be improved by airborne polarimetric measurements performed in different spectral ranges, at different directions of view relative to the sun and at various viewing angles from the horizontal, since there is a polarization contrast between the clean and polluted water surface.
- estimation of soil moisture (Curran 1978, 1979), discrimination between vegetation and soil, classification of different vegetation and soil types, determination of plant/canopy form and orientation (Curran 1982; Buschmann 1993), growth stage estimation of grain crops (Fitch et al. 1984), measurement of the reflection-polarizational characteristics of plant leaves as a function of the leaf surface features (Shul'gin and Moldau 1964; Vanderbilt and Grant 1985a,b; Vanderbilt et al. 1985a,b; Grant et al. 1987a,b; Sarto et al. 1989)
- quality inspection and control of materials during manufacturing, material classification: from the way materials alter the state of polarization of light passing through them, information can be obtained about their crystalline structure or weaknesses (mechanical tensions) in them can be detected.
- discrimination between dielectric and metal materials by illuminating them with light of known polarizational characteristics and measuring the polarization of reflected light (Wolff 1990)
- image segmentation (e.g. quantitative separation of specular and diffuse reflection components), identification of occluding contours, detection of orientation of objects and surfaces (Wolff and Boult 1991)
- polarization-based determination of shape (Koshikawa and Shirai 1987; Jones and Fairney 1989)
- ophthalmology: measurement of the birefringent, dichroic and polarizational characteristics of the ocular media (cornea, lens, vitreous, retina) of the human eye
- polarization-based contrast enhancement (Kalayjian et al. 1996)
- autonomous navigation (Lambrinos et al. 1997)
- robot vision: Consider the problem of an autonomous land vehicle viewing a scene, part of which is reflected by a flat lake or river. How does the vehicle know which are the real elements of the scene? How does a mobile robot know when it is running into a glass door, or if navigating according to edge cues, which are geometric edge cues opposed to specular ones? These non-trivial problems can be solved by using the measured polarization patterns of the scene, because the real objects and their mirror images can be distinguished on

the basis of the differences between their polarizational characteristics (Wolff 1993).
- remote sensing of polarized light in atmospheric physics and meteorology (e.g. Fraser 1968, 1981; Egan and Sidran 1994)

2.1 Different Ways of Qualitative Demonstration of Polarization in the Optical Environment

The presence of linearly or circularly polarized light in the optical environment can be qualitatively demonstrated by the use of a linearly or circularly polarizing filter. Looking through such a filter and rotating it in front of our eyes, the change of intensity of light coming from certain directions may be observed. This intensity change is an unambiguous sign of the polarization of light. If we take colour photographs from a scene through linear polarizers with differently oriented transmission axes and compare them, striking intensity and colour differences may occur in those regions, from which highly polarized light originates, furthermore the brightness and colour contrasts may change drastically between different parts of the scene (Figs. 2.1 and 2.2). This simple way of demonstration of the occurrence of polarized light in nature, that is, translating polarization into brightness and colour shade differences for the human eye, is frequently used in the scientific as well as popular literature (e.g. Wehner 1976, 1982, 1997; Harkness and Wehner 1977; Lythgoe 1979; Schwind 1985b; Können 1985, 1986, 1992; Coulson et al. 1986; Curran 1978, 1979; Land 1993).

Können (1985, 1986, 1992), for instance, published numerous pairs of colour photographs of natural scenes taken through a common linearly polarizing filter directed in such a way that in the first and second picture the polarizer maximally transmitted and extinguished the light from a selected region of the scene, respectively, with the transmission axes perpendicular to each other. In the first picture, where the filter was maximally transmissive, the appearance of the selected region did not differ very much from that viewed with the naked eye, while in the second picture, where the filter was in a direction of maximal extinction, the most striking differences between the scenes viewed with and without a polarizer occurred.

During four Space Shuttle missions Coulson et al. (1986) took photographs about the earth surface with a pair of cameras, both of which contained a linearly polarizing filter with different orientation of the transmission axis. Some qualitative data could have been deduced from the comparison of the obtained picture pairs.

Since for a complete imaging polarimetry at least three "polarizational pictures" are needed if the circular polarization is negligible (see Chapters 2.2, 2.4 and 2.5), these methods are, of course, inappropriate for quantitative measurement of the radiance as well as the degree and angle of linear polarization. The mentioned pairs of polarizational pictures can be considered as the forerunners of imaging polarimetry. If the cited authors had have also taken a third photograph of the

investigated scene with a third orientation of the transmission axis of the polarizer (similarly as in Figs. 2.1 and 2.2), the resulting triplet could have been the basis of an imaging polarimetric evaluation procedure.

Using triangles cut from a sheet of linearly polarizing filter, Karl von Frisch (1953, 1965, 1967) has constructed a simple device, the so-called "Sternfolie" ("star foil"), with which the gross distribution of linear polarization of skylight could be demonstrated (Fig. 2.3). This pioneering instrument was used by Frisch to investigate qualitatively the degree and angle of linear polarization of skylight, which was important to interpret the results of his behavioural experiments with honeybees. Wehner (1976, 1982, 1997), Harkness and Wehner (1977) as well as Lythgoe (1979), for example, took photographs of the full sky by using a 180^{o} field-of-view fisheye lens equipped with a linear polarizer to portray qualitatively the celestial polarization pattern for different solar elevations, as did Können (1985) in his book on polarized light in nature.

A linear polarizer with constant direction of its transmission axis must be rotated in front of the eye in order to perceive the change of intensity of transmitted light if the incident light is polarized. Then the angle of polarization of light coming from a given direction of view can be estimated by finding that orientation of the known transmission axis, at which the transmitted light is the brightest. There is, however, a simpler way to find the E-vector direction. Using a so-called "radial linearly polarizing filter" (the transmission axis of which runs along concentric circles rather than along parallel straight lines), the intensity of transmitted light along each circular transmission axis changes sinusoidally for every 180^{o} turn, if the state of partial linear polarization of the incident light beam is the same across the filter. A characteristic cross-shaped brightness pattern is visible looking through such a radial polarizer (see Fig. 2.4A). The centre of the cross coincides with that of the filter, and the darkest and brightest axes of the cross are the directions where the E-vector of linearly polarized incident light is perpendicular and parallel to the circular transmission axes of the filter, respectively. Due to this feature, radial polarization filters are termed often as "axis finders", since the darkest axis of the seen brightness cross tells the orientation of the transmission axis of another common (non-radial) linearly polarizing filter held in front of the radial one. From the cross pattern produced by a radial filter also the degree of linear polarization can be qualitatively estimated: the greater the contrast between the darkest and brightest axes of the cross, the higher the degree of polarization. If the incident light is unpolarized, a homogeneous brightness pattern is seen across a radial filter.

Figure 2.4A shows a photograph of the entire celestial hemisphere taken by Wehner (1994b, 1997, 1998) with the use of a set of 41 axis-finders, which were mounted on a transparent Plexiglas dome (Fig. 2.4B). Wolff (1993) suggested to build a low-cost "one-big-pixel polarization camera", using such an axis-finder to automate the computation of the state of partial linear polarization of light. A radial filter makes it possible to simultaneously measure the angle of polarization as well as the maximum and minimum of transmitted intensity, from which the degree of linear polarization can be derived.

Some of the above examples demonstrate also the need of quantitative information about the distribution of polarization over the whole sky, for instance. Until only such qualitative techniques and point-source scanning polarimeters existed, the polarization pattern of the whole sky under a given meteorological situation could not have been measured. Thus, earlier the distribution of polarization over the full sky could be represented only by maps obtained either by numerical simulations (Fig. 2.5), or by gathering and averaging data from the sky during an extended period restricted to certain advantageous meteorological conditions (e.g. clear skies). The polarization pattern of the entire sky at a given, often quickly changing atmospheric situation can be measured only by simultaneous full-sky imaging polarimetry, the most novel technique of recent development (Horváth et al. 2002a).

What could have been demonstrated only qualitatively by Frisch (1953, 1965, 1967) with his "Sternfolie", or by Wehner (1976, 1982, 1994b, 1997, 1998), Harkness and Wehner (1977), Lythgoe (1979) and Können (1985) by their fisheye photographs, nowadays can already be measured quantitatively by different kinds of full-sky imaging polarimeters developed by North and Duggin (1997), Voss and Liu (1997), Liu and Voss (1997), Gál et al. (2001a,b,c), Pomozi et al. (2001a,b), Horváth et al. (2002a,b, 2003) as well as Barta et al. (2003). Figures 7.4.4 and 7.4.7 show two examples for the visualization of the polarization pattern of the whole sky measured by full-sky imaging polarimetry. Figures 2.3-2.5, 7.4.4 and 7.4.7 demonstrate well the advance of polarimetry happened in the last 50 years.

2.2 Elements of the Stokes and Mueller Formalism of Polarization

Polarized light can be decomposed into two components vibrating coherently (that is, with a constant phase difference) and perpendicularly to each other. The state of polarization of transversal electromagnetic waves (e.g. light) is usually described by a four-element vector known as Stokes vector $\underline{S}$, first introduced by Stokes (1852) with the following components:

$$\begin{aligned} \underline{S} &= (I, Q, U, V), \\ I &= I_r + I_p = I_{45} + I_{135} = I_{rc} + I_{lc}, \\ Q &= I_r - I_p = I \cdot p \cdot \cos(2\varepsilon) \cdot \cos(2\alpha), \\ U &= I_{45} - I_{135} = I \cdot p \cdot \cos(2\varepsilon) \cdot \sin(2\alpha), \\ V &= I_{rc} - I_{lc} = I \cdot p \cdot \sin(2\varepsilon), \end{aligned} \tag{2.1}$$

where I is the total intensity of light, I_r and I_p are the intensities of the light components polarized totally linearly in a reference plane and perpendicularly to it, I_{45} and I_{135} are the intensities of the components polarized totally linearly in

planes 45° and 135° to the reference plane, I_{rc} and I_{lc} are the intensities of the components polarized circularly right- and left-handed, p is the degree of linear polarization, ε is the ellipticity of polarization, and α is the angle of polarization, which is the angle of the direction of oscillation from a given plane. Q quantifies the fraction of linear polarization parallel to the reference plane, U gives the proportion of linear polarization at 45° with respect to the reference plane, and V quantifies the fraction of right-handed circular polarization. The degree of polarization P, the degree of linear polarization p, the angle of polarization α and the ellipticity ε can be expressed by the components of the Stokes vector as follows (Shurcliff 1962):

$$\begin{aligned} P &= (Q^2 + U^2 + V^2)^{1/2}/I, \quad 0 \le P \le 1, \\ p &= (Q^2 + U^2)^{1/2}/I, \quad 0 \le p \le 1, \\ \alpha &= 0.5 \cdot \arctan(U/Q), \\ \varepsilon &= 0.5 \cdot \arcsin[V/(Q^2+U^2+V^2)^{1/2}]. \end{aligned} \tag{2.2}$$

For partially polarized light the Stokes vector $\underline{S}$ can be decomposed into two vectors, a completely unpolarized vector $\underline{S}_u$ and an elliptically polarized one $\underline{S}_e$:

$$\underline{S} = \underline{S}_u + \underline{S}_e; \quad \underline{S}_u = [I-(Q^2+U^2+V^2)^{1/2}, 0, 0, 0]; \quad \underline{S}_e = [(Q^2+U^2+V^2)^{1/2}, Q, U, V]. \tag{2.3}$$

A change in the state of polarization of light produced by an optical system, that is, a transformation of the Stokes vector $\underline{S}_0 = (I_0, Q_0, U_0, V_0)$ of the incident light into a new Stokes vector $\underline{S} = (I, Q, U, V)$ by an optical process (e.g. reflection, refraction, scattering, diffraction, birefringence, optical activity) can be expressed as a linear transformation in a four-dimensional space:

$$\underline{S} = \mathbf{M} \cdot \underline{S}_0, \tag{2.4}$$

where $\boldsymbol{M}$ is a four-by-four matrix called "Mueller matrix" with real elements M_{ij} (i,j=0,1,2,3) containing information on all polarization properties of light. In general, the matrix element M_{00} represents the intensity of the emergent light when unpolarized ($P = p = 0$) light is entering the system. Elements M_{01}, M_{02}, M_{03} describe the diattenuation or dichroism, and M_{10}, M_{20}, M_{30} characterize the polarizance. The lower 3×3 submatrix with elements M_{kl} (k,l=1,2,3) contains the retardation. The 16 elements of the Mueller matrix of a given optical system can be obtained by 16 measurements with independent combinations of states of polarization (degrees and angles of linear and circular polarization) of the incident light. The degree of polarization P in the Mueller formalism is (Azzam and Bashara 1992):

$$P = [(\Sigma - M_{00}^2)/3]^{1/2}/M_{00}, \qquad \text{where } \Sigma = \sum_{i,j=0}^{3} M_{ij}^2. \tag{2.5}$$

If the incident light is unpolarized, the degree of polarization of transmitted light, called polarizance or polarizing power *PO* is (Collett 1994):

$$PO = [(M_{10}^2+M_{20}^2+M_{30}^2)/M_{00}^2]^{1/2}, \quad 0 \le PO \le 1,$$

$$\underline{PO} = (PO_1, PO_2, PO_3), \quad PO_i = M_{i0}/M_{00}, \quad i = 1, 2, 3, \tag{2.6}$$

where $\underline{PO}$ is the polarizance vector.

2.3 Principle of Polarimetry with Polarization-Insensitive Detectors

Consider an optical instrument with elements such as imaging lenses, spectral filters, polarizers, quarter-wave plates and/or birefringent crystals, for instance. In general, this instrument may cause absorption, scattering, reflection, refraction, diffraction, birefringence, and so on. These actions are represented by the system Mueller matrix $\boldsymbol{M}$, and the change of the Stokes vector $\underline{S_0(I_0,Q_0,U_0,V_0)}$ of incident light to $\underline{S(I,Q,U,V)}$ of transmitted light is described by Eqn. (2.4). If a polarization-insensitive detector, e.g. a photoemulsion or a charge-coupled device (CCD) with the light at approximately normal incidence, is placed behind the optical system, then only the intensity $I = M_{00}\cdot I_0 + M_{01}\cdot Q_0 + M_{02}\cdot U_0 + M_{03}\cdot V_0$ of light exiting the system can be measured. If the elements M_{00}, M_{01}, M_{02} and M_{03} in the first row of the system Mueller matrix are known and variable, the Stokes vector $\underline{S_0}$ of the incoming light can be determined in four measurements, in which the intensities I_1, I_2, I_3 and I_4 are registered for four independent and known combinations of polarizational states of the incident light. The states of polarization of incoming light can be changed by varying the orientation of the polarizer's transmission axis, for instance. Then the system of equations

$$\begin{aligned}
I_1 &= M_{00}^{(1)}\cdot I_0 + M_{01}^{(1)}\cdot Q_0 + M_{02}^{(1)}\cdot U_0 + M_{03}^{(1)}\cdot V_0,\\
I_2 &= M_{00}^{(2)}\cdot I_0 + M_{01}^{(2)}\cdot Q_0 + M_{02}^{(2)}\cdot U_0 + M_{03}^{(2)}\cdot V_0,\\
I_3 &= M_{00}^{(3)}\cdot I_0 + M_{01}^{(3)}\cdot Q_0 + M_{02}^{(3)}\cdot U_0 + M_{03}^{(3)}\cdot V_0,\\
I_4 &= M_{00}^{(4)}\cdot I_0 + M_{01}^{(4)}\cdot Q_0 + M_{02}^{(4)}\cdot U_0 + M_{03}^{(4)}\cdot V_0
\end{aligned} \tag{2.7}$$

has to be solved for I_0, Q_0, U_0 and V_0. These equations form the basis of the analyser-type polarimeters using intensity detectors, called radiometers. What must be determined through the calibration process are the elements $M_{00}^{(i)}$, $M_{01}^{(i)}$, $M_{02}^{(i)}$, $M_{03}^{(i)}$ (i=1,2,3,4) in the first row of the Mueller matrix with each orientation

of the transmission axis of the polarizer. For example, if a linearly polarizing filter is used as polarizer, its Mueller matrix is (Voss and Liu 1997):

$$\begin{aligned}
&M_{00} = t+\tau, \quad M_{01} = (t-\tau)\cos 2\beta, \quad M_{02} = (t-\tau)\sin 2\beta, \quad M_{10} = (t-\tau)\cos 2\beta,\\
&M_{11} = (t+\tau)\cos^2 2\beta + 2(t\tau)^{1/2}\sin^2 2\beta, \quad M_{12} = [t+\tau-2(t\tau)^{1/2}]\cos 2\beta \sin 2\beta,\\
&M_{20} = (t-\tau)\sin 2\beta, \quad M_{21} = [t+\tau-2(t\tau)^{1/2}]\cos 2\beta \sin 2\beta,\\
&M_{22} = (t+\tau)\sin^2 2\beta + 2(t\tau)^{1/2}\cos^2 2\beta, \quad M_{33} = 2(t\tau)^{1/2}\\
&M_{03} = M_{13} = M_{23} = M_{30} = M_{31} = M_{32} = 0,
\end{aligned} \tag{2.8}$$

where t and τ are the transmittances of the polarizer along the transmission axis and perpendicularly to it, and β is the angle of the transmission axis relative to a reference plane. If a sequence of perfect ($t = 1$, $\tau = 0$) linear polarizers with say $\beta = 0^o$, 45^o, 90^o are used as analysers for the Stokes vector $\underline{S_0} = (I_0, Q_0, U_0, V_0)$ of incoming light, then using Eqns. (2.7) and (2.8), the intensities measured by a detector after the polarizers are

$$I_1(\beta=0^o) = I_0 + Q_0, \qquad I_2(\beta=45^o) = I_0 + U_0, \qquad I_3(\beta=90^o) = I_0 - Q_0. \tag{2.9}$$

From this system of equations the elements I_0, Q_0 and U_0 of the Stokes vector of incoming light can be determined. If the Stokes parameter V_0, characterizing the fraction of circular polarization, is also required, then a fourth measurement, using a circular polarizer as an analyser, is needed.

2.4 Polarimetry of Circularly Unpolarized Light by Means of Intensity Detectors

Light in the natural optical environment is usually not circularly polarized. The few known exceptions are listed and discussed in the book of Horváth and Varjú (2003). Skylight polarization, for instance, is predominantly linear and the component of circular polarization of skylight can be neglected (Hannemann and Raschke 1974). Thus the contribution of the Stokes parameter V characterizing circular polarization to the total intensity is negligible in comparison with that of the linearly polarized component. In other words, the minimal degree of circular polarization V/I of light in nature can be generally ignored. The remaining Stokes vector components I, Q and U, components of the so-called "partial Stokes vector", can be determined from three intensity measurements, using a rotating linear polarizer in front of a radiometer, for instance. If these three measurements happen with angles of orientation $\beta = 0^o$, 60^o and 120^o of the transmission axis of a perfect polarizer, for example, and the state of polarization of light is not changed by other components of the polarimeter, then the transmitted intensities I are the following (Prosch et al. 1983):

$$I(\beta=0^o) \equiv I_0 = I_i\cdot[1 + p\cdot\cos(2\alpha)]/2,$$
$$I(\beta=60^o) \equiv I_{60} = I_i\cdot[1 - 0.5\cdot p\cdot\cos(2\alpha) + 0.5\cdot p\cdot 3^{1/2}\cdot\sin(2\alpha)]/2,$$
$$I(\beta=120^o) \equiv I_{120} = I_i\cdot[1 - 0.5\cdot p\cdot\cos(2\alpha) - 0.5\cdot p\cdot 3^{1/2}\cdot\sin(2\alpha)]/2, \quad (2.10)$$

where I_i is the intensity of incident light. The components Q_i and U_i of the incident Stokes vector are:

$$Q_i = 2(2I_0 - I_{60} - I_{120})/3,$$
$$U_i = -2(I_{120} - I_{60})\cdot 3^{-1/2}. \quad (2.11)$$

Finally, the intensity I_i, degree of linear polarization p and angle of polarization α of incident light can be calculated as follows:

$$I_i = 2(I_0 + I_{60} + I_{120})/3, \qquad p = (Q_i^2+U_i^2)^{1/2}/I_i, \qquad \alpha = 0.5\cdot\text{arc tan}(U_i/Q_i). \quad (2.12)$$

2.5 Point-Source, Scanning and Imaging Polarimetry

The major aim of polarimetry is to measure the four components I, Q, U and V of the Stokes vector $\underline{S}$, from which further quantities of the incident light can be derived, according to Eqn (2.2). These measurements can be done either by a point-source polarimeter or by an imaging one. The only principal difference between them is that the former performs measurements in a given direction representing a very narrow field of view within which the optical variables I, Q, U and V are averaged, while the latter measures the polarization simultaneously in many directions in a wide field of view.

There is an intermediate technique, the scanning point-source polarimetry between these two extrema. Such a polarimeter scans a given area of the optical environment and measures sequentially the polarization in many directions (Fig. 2.6). If there is no temporal change of polarization, a polarization pattern obtained by imaging polarimetry can also be measured equivalently by scanning point-source polarimetry. However, scanning a greater area of the optical environment with a point-source polarimeter is a troublesome and time-consuming task, which generally can be performed only in the laboratory using complicated, computer-controlled procedures. It is, therefore, not surprising that this technique has been used only sporadically (e.g. Shaw 1975; Brines and Gould 1982).

Using imaging polarimetry, the spatial distribution of polarization can be easily and quickly determined. The need to receive polarized optical information pixel-by-pixel from a wide field of view has resulted in the rapid development of imaging polarimetry in the 1980's, 1990's and early 2000's. This technique has

been used for different purposes in computer vision (e.g. Wolff 1993), in atmospheric remote sensing (e.g. Walraven 1981; Prosch et al. 1983; Egan 1986; Deschamps et al. 1994; North and Duggin 1997; Voss and Liu 1997; Horváth et al. 1998b, 2002a,b, 2003; Horváth and Wehner 1999; Gál et al. 2001a,c; Pomozi et al. 2001a,b; Barta et al. 2003), and in biology (e.g. Shashar et al. 1995a,b; Horváth and Zeil 1996; Horváth and Varjú 1997; Horváth et al. 1997, 1998a, 2002c; Kriska et al. 1998; Bernáth et al. 2001b, 2002, 2003).

2.6 Sequential and Simultaneous Polarimetry

If the (at least necessary) 3 intensity measurements with different orientations of the transmission axis of the polarizer are performed one after the other, we speak about "sequential polarimetry". When all these measurements happen at the same time, it is called "simultaneous polarimetry". For the latter at least 3 separate polarimeters are needed. The advantage of simultaneous polarimetry is, that also temporally changing radiation fields (e.g. light from cloudy skies with rapidly moving clouds, or skylight after sunset or prior to sunrise, or measurements from a moving platform) can be measured with it, if the time of measurement is not longer than the characteristic period during which considerable changes occur in the radiation field. Its disadvantage is that at least 3 polarimeters have to be handled simultaneously, which is not a simple task, furthermore such a group of polarimeters is heavy, voluminous, its setting up, dismounting and transferring is difficult and time-consuming. These disadvantages make frequently impossible the use of simultaneous polarimetry in the field.

The disadvantage of sequential polarimetry is that temporally changing radiation fields cannot be measured with it. Its advantage is, that only one polarimeter has to be handled, the setting up, dismounting and transferring of which is much easier and quicker. In the field, the polarization of certain optical phenomena – like rainbows (Barta et al. 2003), for example, the occurrence of which is accidental – can practically be measured only with a simple and portable sequential polarimeter, which can be set up quickly anywhere and at any time. The advantage of a sequential polarimeter against a heavy simultaneous polarimeter composed of several separate parts has been experienced, for instance during the first observation of the fourth neutral polarization point in the atmosphere (Horváth et al. 2002b), when the polarization of the upwelling earthlight has been measured by a simple sequential polarimeter in the gondola of a hot air balloon. This measurement could not have been performed by a heavy, voluminous simultaneous polarimeter.

2.7 Colour Coding and Visualization of Polarization Patterns

On the basis of the functional similarity between polarization vision and colour vision, Bernard and Wehner (1977) suggested a hue-saturation-brightness visualization method for partially linearly polarized light. This "composite visualization" scheme was used by Wolff and collaborators (e.g. Wolff 1993; Cronin et al. 1994; Shashar et al. 1995a), for example, who coded the measured angle of polarization α, degree of linear polarization p and intensity I of partially linearly polarized light by the hue, saturation and brightness, respectively. In their polarization maps, unpolarized light appears achromatic, strongly polarized regions show up chromatically saturated, and the intensity of light is the brightness regardless of colour. The advantage of this visualization lies in its compactness: it displays the distribution of all three optical parameters (I, p, α) in a single, false-coloured picture. The disadvantage of this coding is, that it is difficult to decompose, since in a complex false-coloured picture it is not easy to separate and decode the values of I, p and α from each other. Changes in hue (coding α) appear to the human visual system more strikingly than changes in saturation (coding p), furthermore the perception of the hue-saturation-brightness scale is very non-linear (Shashar et al. 1995a).

The latter problem does not occur if the distributions of I, p and α are displayed in three separate patterns with arbitrary unambiguous colour coding. This "separate visualization" of the I-, p- and α-patterns is preferred by Horváth and collaborators, for instance (e.g. Horváth and Varjú 1997; Horváth and Wehner 1999; Gál et al., 2001c; Pomozi et al. 2001b; Barta et al. 2003; Bernáth et al. 2002), for instance.

Other authors (e.g. Dürst 1982; Sivaraman et al. 1984; Liu and Voss 1997; Gabryl et al. 1998) display the I-, p- or α-patterns measured by imaging polarimetry in the form of the conventional contour plots used frequently in the cartography, for example. Although this "contour plot visualization" is the most traditional, it can hardly reproduce the image feature of the spatial distribution of polarization, which is the most important characteristic of data gained by imaging polarimetry.

2.8 Field of View of Imaging Polarimetry

The field of view of an imaging polarimeter is limited by that of the imaging optics used. In the case of common photographic and video cameras, the field of view of the lens system is about 30^o-50^o (horizontal) $\times$ 20^o-40^o (vertical) depending on the focal length and the aperture. This common field of view can be extended e.g. by decreasing the focal length. A fisheye lens with 8 mm focal length mounted onto a normal photographic camera is an extremum, ensuring a

conical field of view with an aperture angle of 180°, by which the whole hemisphere of the optical environment can be imaged.

As an alternative, a 180° field-of-view fisheye lens can be replaced by a spherical mirror with a 180° field of view, and the camera can be suspended by a holder above the mirror. A similar construction is used in the TS-990 Total Sky Imager (Fig. 2.7) produced by the Yankee Environmental Systems Inc. (YES 2001) and used to detect radiometrically the clouds (see Chapter 7.7), or in the full-sky imaging polarimeter (Fig. 5.1) designed by North and Duggin (1997). 180° field-of-view imaging polarimetry is ideal to study the polarization patterns of the full sky or the reflection-polarization patterns of water surfaces (Fig. 2.8), for instance.

2.9 Narrow Field-of-View Imaging Polarimetry with Photographic Technique

Walraven (1977) has as first demonstrated by simple photographic technique that the state of polarization is a valuable parameter for identifying different ground targets, aerosol and dust layers as well as the water phase of clouds.

2.9.1 A Forerunner of Imaging Polarimetry Using Savart Filter

One of the forerunners of the development of imaging polarimetry was Gerharz (1976), who measured the polarization of the circumsolar scatter field in a field of view of 12°×15° during the total solar eclipse on 7 March 1970. He photographed the scene by a 30 cm focal length camera through external objective filters consisting of a modified Savart polariscope and an interference filter (535 nm). On the negatives dark interference bands with low contrast have been produced, which extended through almost the entire field of view. These bands originate from the scattered polarized skylight that had been intercepted by the filters before entering the camera. The contrast of the bands is a measure of the degree of linear polarization p: the greater the contrast, the higher is p. The exposed plates were analysed by a microdensitometer and indicated a maximum p of 2.5% in the immediate solar vicinity. The mechanism of the formation of interference bands by a Savart filter and the evaluation of the contrast of these bands are described in detail by Gerharz (1975).

2.9.2 Simultaneous Photographic Polarimeter

Fitch et al. (1984) designed a simultaneous imaging photopolarimeter, which makes four photographs of a scene through linear polarizers with four different directions (0°, 45°, 90° and 135°) of the transmission axis relative to a reference

direction. With this polarimeter the polarization of light reflected from grain crops was studied during the heading growth stage.

2.9.3 Sequential Photographic Polarimeters

Solar physicists and astronomers have also developed different imaging polarimetric techniques for the ground-based measurement of the polarization pattern of the solar corona during total solar eclipses (see Chapter 9.3). One of the first astronomers using imaging polarimetric technique for this purpose was Dürst (1982), who took sequential photographs about the corona during the solar eclipse of 16 February 1980. He used a camera with 370 mm focal length equipped with six neutral density filters, one colour (600 nm) filter and one linearly polarizing filter mounted between glass plates in front of the objective with four orientations of the transmission axis 45^o apart. After digitisation by an automatic microdensitometer and evaluation of the four polarizational pictures taken sequentially from the corona, two-dimensional maps of the degree p and angle α of linear polarization of the corona light were obtained. There are two possibilities for analysing these data:

1. The first uses all four exposures together leading to p and α.
2. The second assumes that the polarization of the so-called K-corona is produced by Thomson scattering of light on free electrons and therefore the E-vector of the corona light is perpendicular to the radial scattering plane. In this case only two exposures with 90^o difference in the orientation of the transmission axes of the polarizers are combined to obtain p.

Sivaraman et al. (1984) measured the polarization pattern of the solar corona during the total eclipse on 16 February 1980 with the use of a four-lens camera (focal length = 1 m) equipped with linearly polarizing sheets with four different orientations of their transmission axes 45^o apart. The polarizational photographs were digitised by a microdensitometer. Later, similar photopolarimetric methods were routinely used in the investigation of the polarization of the solar corona during eclipses (e.g. Gabryl et al. 1998).

Lee (1998a) designed a rotating-analyzer sequential photographic polarimeter and estimated with it the approximate values of the degree p of linear polarization of light from the clear sky near sunset at inland and coastal sites. He also observed the Arago and Babinet neutral points in the resulting approximative p-maps. His method used only two digitised pictures of colour slides taken from a scene through a linearly polarizing filter with two orthogonal directions of the transmission axis. These two directions were the directions that gave the brightest and darkest image as measured by the camera's light meter. He also demonstrated that more reliable results are obtained if four photographs are taken through a linearly polarizing filter with four different (0^o, 45^o, 90^o, 135^o) directions of the transmission axis.

Table

Table 1.1. The most important properties of some imaging polarimeters designed by different authors and used for various purposes. Since all instruments contain linearly polarizing filter(s) of different types, the polarizers are not mentioned and specified in the column "imaging optics" (IO). *1D*: one-dimensional (linear). *B*: binned. *CAMO*: camera optics. *CCD*: charge-coupled device. *CF*: colour filter. *CIR*: circular. *D*: digital. *DET*: detector. *DPLSM*: differential polarization laser scanning microscopy. *FEL*: fisheye lens. *FIP*: forerunner of imaging polarimetry. *FOV*: field of view. *IR*: infrared ($\lambda > 750$ nm). *IT*: imaging tube. *MMI*: Mueller matrix imaging polarimeter. *NF*: neutral density filter. *PCC*: polarization camera chip. *PE*: photoemulsion. *PEM*: piezoelastic modulator. *PHO*: photopolarimeter. *POR*: portable. *PP*: photographic plate. *PPBS*: polarizing plate beam-splitter. *PSC*: polarization-sensitive chip. *RES*: spatial resolution (pixel × pixel). *SEQ*: sequential. *SIM*: simultaneous. *SR*: spectral region (nm). *STE*: stereo. *STO*: imaging Stokes polarimeter. *SUB*: submersible. *TNLC*: twisted-nematic liquid crystal. *UV*: ultraviolet. *V*: video. *VID*: video polarimeter. *VIS*: visible (400–750 nm). *WL*: white light.

Author(s)	Type	IO	DET	FOV	RES	SR	Application
Gerharz (1976)	FIP	CAMO + Savart filter + CF	PP	12×15°	–	535	Polarization distribution of the circumsolar scatter field during a total solar eclipse
Dürst (1982)	SEQ PHO	CAMO + 6 NF + 1 CF	PE	8×10°	50×50	600	Polarization pattern of the solar corona during a total solar eclipse
Prosch *et al.* (1983)	SIM VID	3 lens systems	IT	25×25°	36×36	VIS	Ground- and air-borne remote sensing of landscape features
Sivaraman *et al.* (1984)	SIM PHO	four-lens CAMO	PE	3×3°	32×32	WL	*p*-pattern of the solar corona during a total solar eclipse
Fitch *et al.* (1984)	POR SEQ PHO	CAMO	PE	30×40°	512×512	VIS	Polarization pattern of light reflected from grain crops during the heading growth stage
POLDER (1994-1997) Deschamps *et al.* (1994)	SEQ VID	wide field-of-view optics + filter wheel	CCD	114× 114°	242×274	443, 670, 865	Space-borne measurement of the polarizational characteristics of earthlight
Wolff (1993), Cronin *et al.* (1994), Shashar *et al.* (1995a, 1996)	SEQ VID SUB	CAMO + 2 TNLC	CCD	30×40°	165×192 (D) 240×320 (V)	VIS	Polarization patterns of objects and biotopes
Wolff (1994), Wolff & Andreou (1995)	SEQ VID	2 CAMO + PPBS + TNLC	CCD	20×20°	165×192	VIS	Polarization patterns of objects for robot vision
Wolff & Andreou (1995)	1D SIM PCC	lens system	PSC	-	3×128	VIS	Prototype of future 2D polarization camera chips
Povel (1995)	SIM STO	telescope + PEMs	CCD	0.42'× 0.83'	288×385	VIS	Observation of solar magnetic fields
Pezzaniti & Chipman (1995)	MMI SEQ	lens system + retarders + laser	CCD	42×42°	512×512	VIS+ IR	Polarizational properties of static optical systems and samples
North & Duggin (1997)	SIM PHO	four-lens CAMO + spherical mirror	PE	180° CIR	300×300	VIS	Ground-borne measurement of skylight polarization
Voss & Liu (1997)	SEQ VID	FEL	CCD	178° CIR	528×528 (B)	VIS	Ground-borne measurement of skylight polarization
Horváth & Varjú (1997)	POR SEQ VID	CAMO	CCD	50×40°	736×560	VIS	Polarization patterns of sky, objects and biotopes
Lee (1998)	POR SEQ PHO	CAMO	PE	36×24°	550×370	VIS	Polarization patterns of clear skies
Horváth & Wehner (1999)	POR SEQ VID	CAMO	UV IT	20×15°	736×560	UV+ VIS	Polarization patterns of sky, objects and biotopes
Bueno & Artal (1999), Bueno (2000)	SEQ MMI	CAMO + 2 TNL + 2 quarter-wave plate + laser	CCD	1×1°	60×60	630	Polarizational properties of static optical systems and samples (e.g. human eye)
Hanlon *et al.* (1999)	SIM VID	3-tube CAMO + prismatic beam-splitter	IT	20×30°	512×384	VIS	Polarization patterns of moving animals

Author(s)	Type	IO	DET	FOV	RES	SR	Application
Mizera *et al.* (2001)	POR SEQ STE VID	CAMO	CCD	50×40°	736×560	VIS	Polarization patterns of objects and biotopes
Gál *et al.* (2001c)	POR SEQ PHO	FEL + filter wheel	PE	180° CIR	670×670	VIS	Ground- and air-borne measurements of polarization patterns of the atmosphere, objects and biotopes
Shashar *et al.* (2001)	SEQ VID	microscope	CCD	5×5°	512×384	VIS	Polarization patterns of microscopic targets
Horváth *et al.* (2002a)	POR SIM PHO	3 FEL	PE	180° CIR	670×670	VIS	Ground-borne measurements of skylight polarization
Pomozi (2002), Pomozi *et al.* (2003), Garab *et al.* (2003)	DPL SM	laser scanning microscope	CCD	256× 256 μm	1024×1024	VIS	Study of the anisotropic architecture of microscopic samples and the interaction of the sample with polarized light

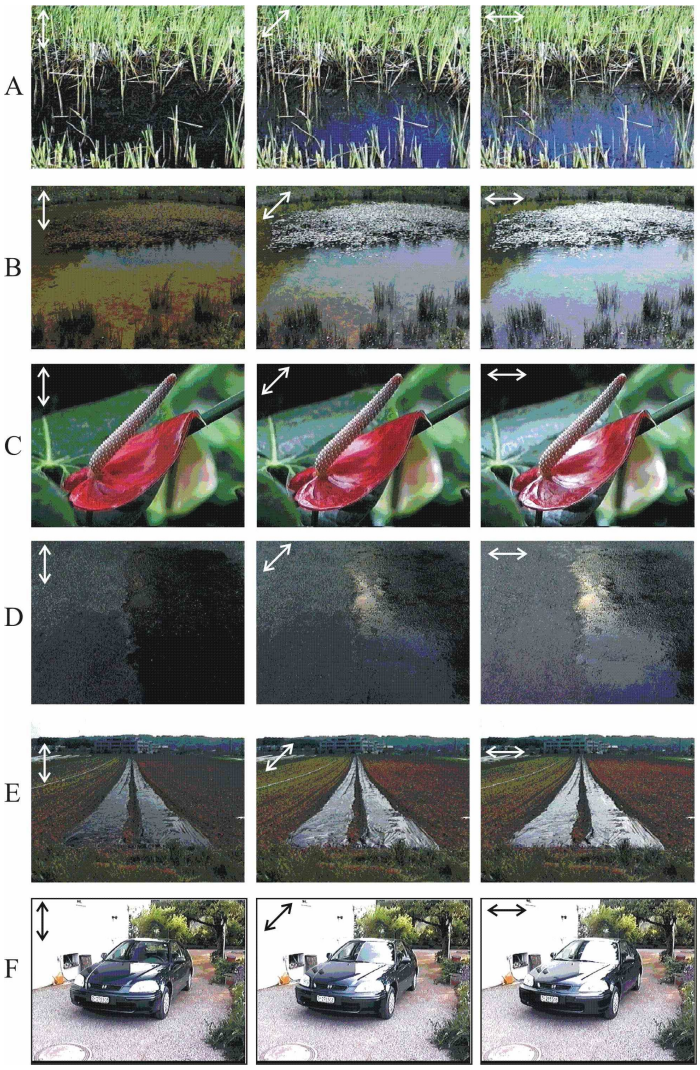

Fig. 2.1. Triplets of colour pictures of various scenes from which highly polarized light originates. The pictures are taken by a video camera through a sheet of linearly polarizing filter with three different orientations of the transmission axis shown by double-headed arrows. A: A dark brown bottomed pond, the surface of which reflects blue light from the clear sky. B: A bright yellow bottomed pond with some plants on its surface under a clear sky. C: The flower of *Epipremnum aureum* (Aracea) possessing a shiny petal-imitating red leaf called spathe. In the background there are shiny green leaves illuminated by light of a full clear sky from above through the glass panes of a greenhouse. D: Surface of a grey asphalt road under a clear sunset sky. The upper half of the road is rough and light grey, the lower half is smooth and dark grey, the left half is dry, the right half is wet. E: Stripes of shiny black plastic sheets used in the agriculture laid onto a plough-land under a clear sky. F: A car under a clear sky.

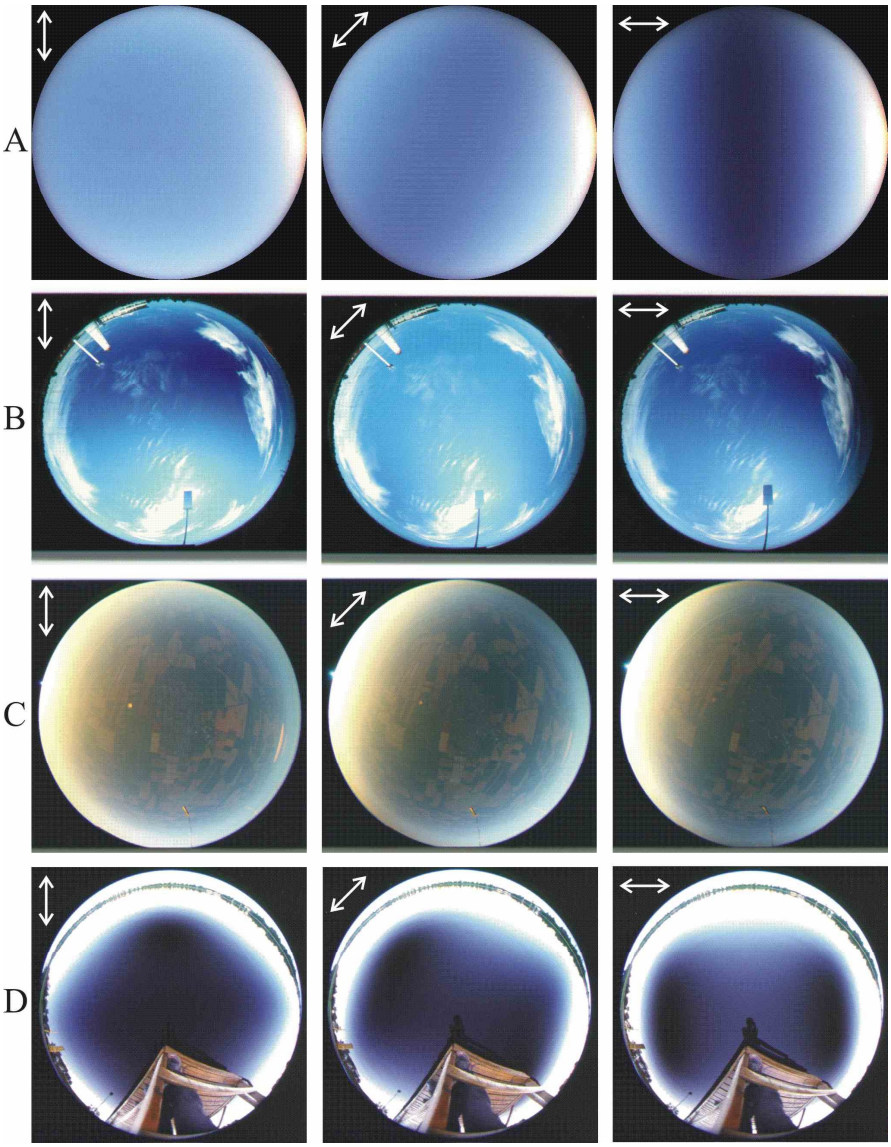

Fig. 2.2. Triplets of colour photographs of various scenes with highly polarized light taken by a 180° field-of-view fisheye lens through a linear polarizer with three different orientations of the transmission axis shown by double-headed arrows. The optical axis of the lens is vertical, the periphery of the circular pictures is the horizon, while the centre is the zenith (A, B) or nadir (C, D). A: A clear sky at sunrise. B: A partly cloudy sky with sun occluded by a metal sheet. C: Sunlight reflected from the ground and scattered in the atmosphere below a hot air balloon photographed at sunrise at an altitude of 4000 m. D: A dark lake with smooth surface photographed at sunset from a jetty.

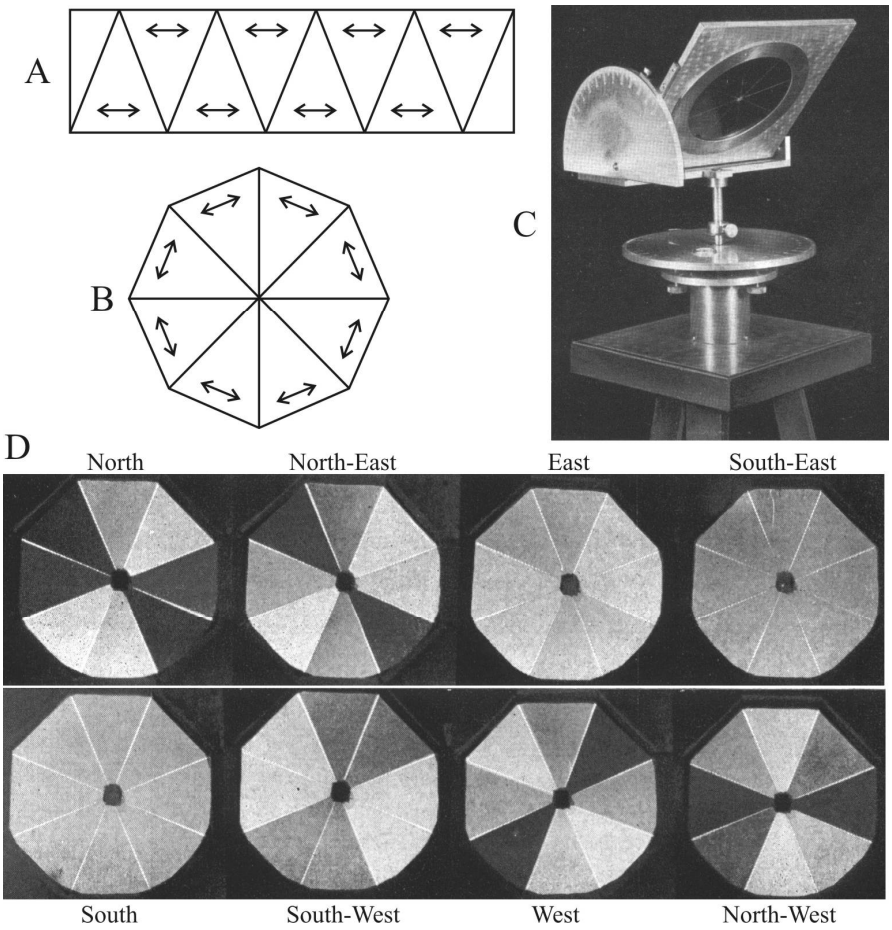

Fig. 2.3. A: Schematic drawing of a sheet of linearly polarizing filter with cut pattern to construct the "Sternfolie" ("star foil") used to demonstrate the gross distribution of linear polarization of skylight by Karl von Frisch (1953, 1965, 1967). The orientation of the transmission axis is shown by double-headed arrows. B: The geometry of the "Sternfolie". C: Simple instrument – a "Sternfolie" mounted onto a metal holder in such a way that both the elevation and azimuth of the viewing direction through the foil can be changed –, with which Frisch (1953, 1965, 1967) investigated qualitatively the polarization of skylight. D: View through the "Sternfolie" in eight different directions in the sky with an angle of elevation of 45^{o}. (After Fig. 59, p. 85; Fig. 69, p. 99, Fig. 70, p. 100 of Frisch 1953).

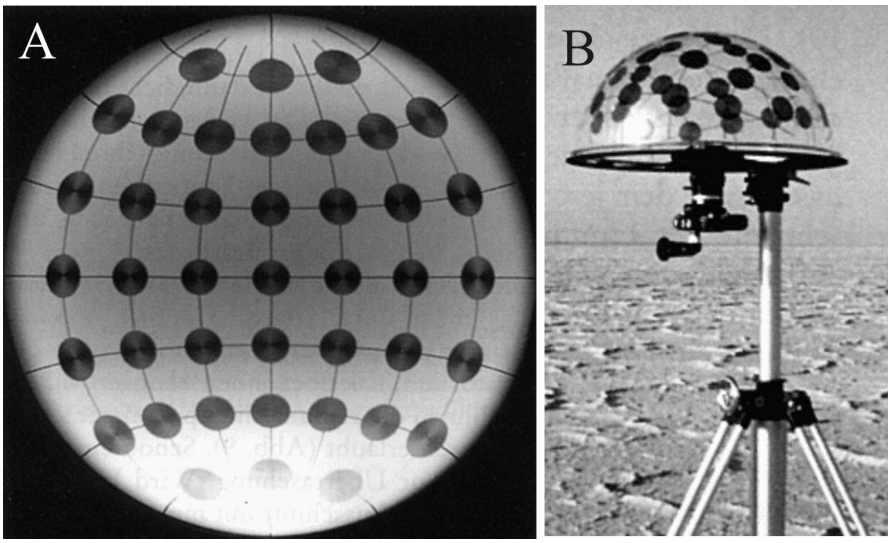

Fig. 2.4. Photograph of the entire sky (A) taken by a 180^{o} field-of-view fisheye lens with the use of a set of 41 circular axis-finders, which were mounted on a transparent Plexiglas dome (B). The dark axis of the cross-shaped brightness pattern seen in the axis-finders gives the E-vector orientation of skylight. (After Fig. 7, p. 15 of Wehner 1994b).

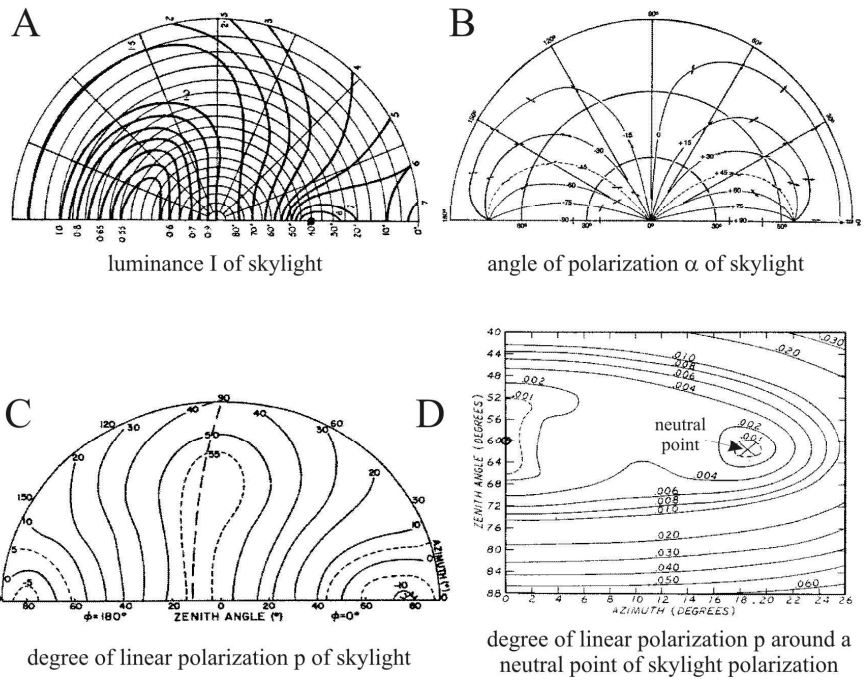

Fig. 2.5. Numerically calculated maps displaying the distribution of luminance I (A, wavelength λ = 312 nm, solar zenith angle θ_s = 50°), angle of polarization α (B, λ = 495 nm, θ_s = 85.4°) and degree of linear polarization p (C, λ = 312 nm, θ_s = 78.5°; D, λ = 550 nm, θ_s = 30°) of light from half of the clear sky. (After Fig. 6.1, p. 335; Fig. 4.36, p. 261; Fig. 4.12, p. 215; Fig. 7.7, p. 392 of Coulson 1988).

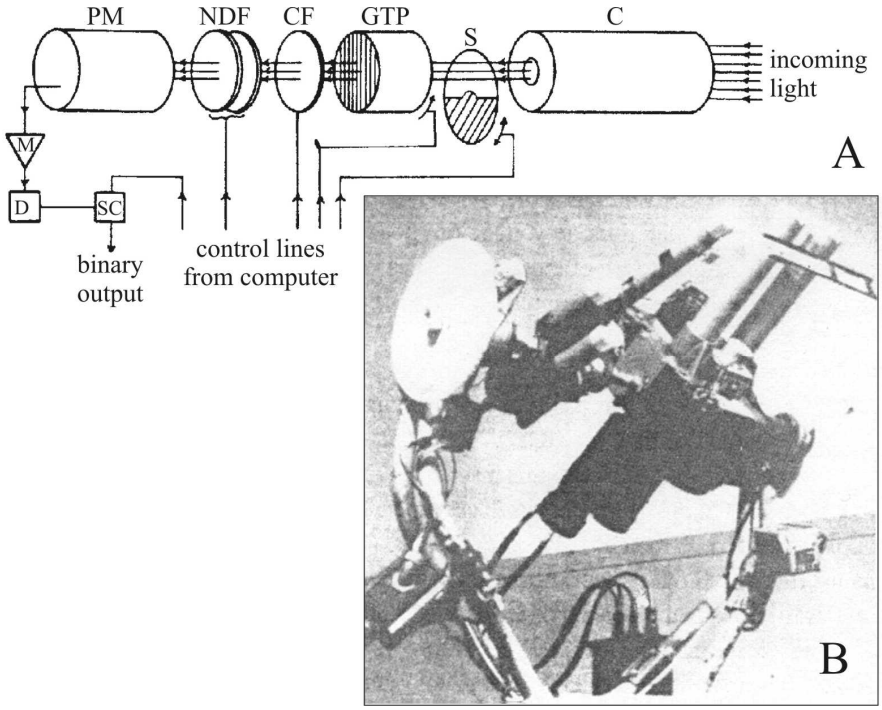

Fig. 2.6. Schematic diagram of a stepped analyser-type non-imaging point-source polarimeter (A). C: collimator tube, S: shutter, GTP: Glan-Thompson prism, CF: colour filter, NDF: neutral density filters, PM: photomultiplier tube, M: amplifier, D: discriminator, SC: scaler. (After Fig. 11.10, p. 556 of Coulson 1988). Photograph of a Seaman-Sekera dual-channel scanning point-source polarimeter (B). (After Fig. 11.11, p. 561 of Coulson 1988).

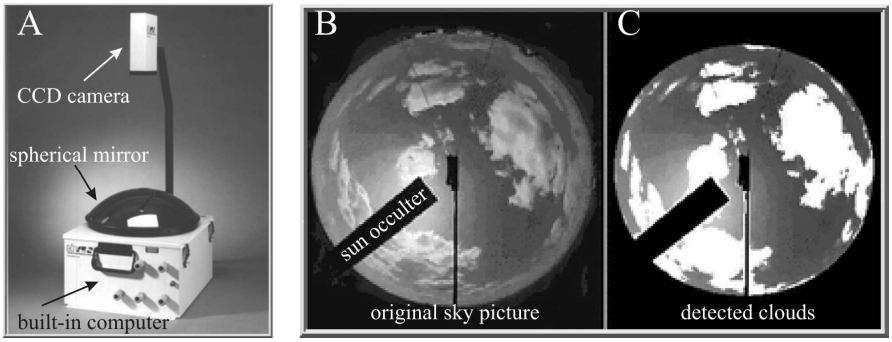

Fig. 2.7. A: The TSI-990 Total Sky Imager with a spherical mirror possessing 180^{o} field of view. B: Picture of a cloudy sky taken by the instrument. C: The clouds (white) and clear sky regions (grey) detected radiometrically by the instrument. (After YES 2001).

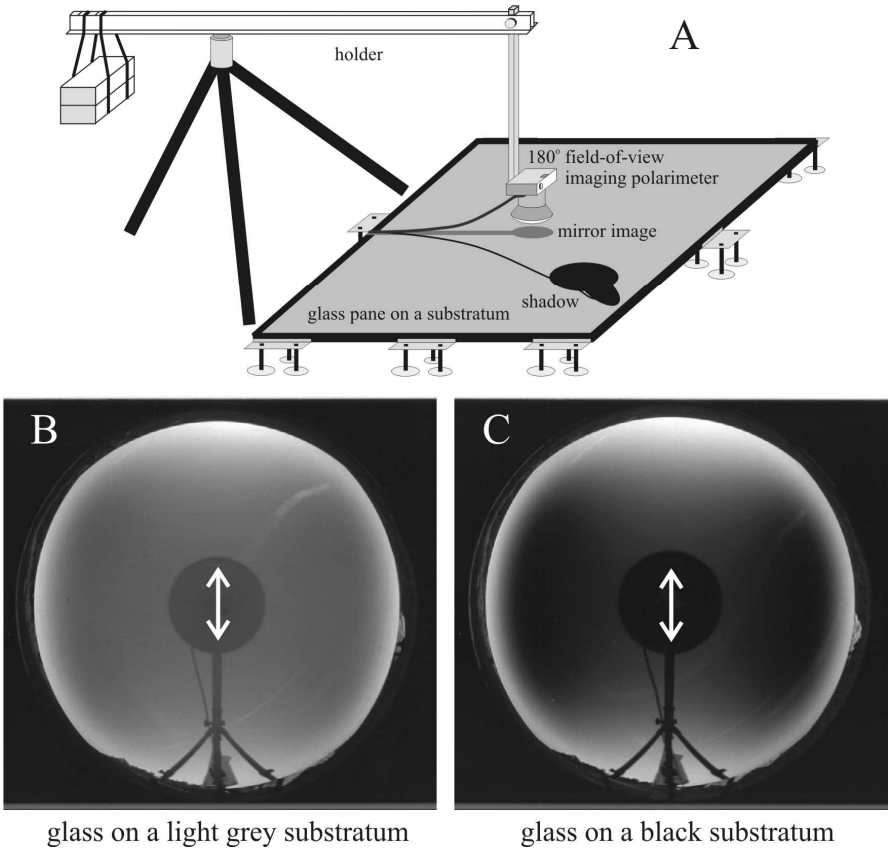

Fig. 2.8. A: The experimental setup used to measure the polarization patterns of skylight reflected from a glass pane by 180° field-of-view imaging polarimetry. B, C: Photographs taken by the 180° field-of-view fisheye lens of the polarimeter from glass on a light grey (B) and black (C) substratum through a linearly polarizing filter, the transmission axis of which is shown by double-headed arrows. (After Fig. 2A of Bernáth et al. 2003).